

GEOLOGICAL  
SURVEY  
OF  
CANADA

DEPARTMENT OF ENERGY,  
MINES AND RESOURCES

*Personal Copy -*

This document was produced  
by scanning the original publication.

Ce document est le produit d'une  
numérisation par balayage  
de la publication originale.

PAPER 67-28

AN AUTOMATIC 3-MAGNET OR  
BIASTATIC MAGNETOMETER

(Report and 8 figures)

A. Larochelle and K. W. Christie



GEOLOGICAL SURVEY  
OF CANADA

PAPER 67-28

AN AUTOMATIC 3-MAGNET OR  
BIASTATIC MAGNETOMETER

A. Larochelle and K. W. Christie

DEPARTMENT OF ENERGY, MINES AND RESOURCES

© Crown Copyrights reserved

Available by mail from the Queen's Printer, Ottawa,  
from the Geological Survey of Canada,  
601 Booth St., Ottawa  
and at the following Canadian Government bookshops:

OTTAWA

*Daly Building, Corner Mackenzie and Rideau*

TORONTO

*221 Yonge Street*

MONTREAL

*Æterna-Vie Building, 1182 St. Catherine St. West*

WINNIPEG

*Mall Center Bldg., 499 Portage Avenue*

VANCOUVER

*657 Granville Street*

or through your bookseller

A deposit copy of this publication is also available  
for reference in public libraries across Canada

Price, \$1.50      Cat. No. M44-67-26

*Price subject to change without notice*

ROGER DUHAMEL, F.R.S.C.  
Queen's Printer and Controller of Stationery  
Ottawa, Canada

1967

CONTENTS

	Page
Abstract .....	v
Introduction .....	1
Part I - Theoretical considerations .....	1
Stability of the biastatic system.....	2
Limit of resolution of the biastatic system.....	7
Part II - The Geological Survey instrument .....	11
Description .....	11
Calibration and operation .....	20
Summary and conclusion.....	27
Acknowledgments .....	27
Bibliography .....	28

---

Table I. Expression of fields at $p_0$ , $p_1$ and $p_2$ due to Dipole P .....	7
II. 16 orthogonal positions of dipole P relatively to axes X', Y and Z' .....	16
III. Instrument Constant Determinations for different values of "d" .....	21
IV. Repeated Magnetization Measurements on a 22.6 cc cylindrical specimen at $d = 6$ cms .....	22
V. Statistical Parameters of Test Results .....	23
VI. Statistical Angular Parameters of Test Results .....	23

Illustrations

Figure 1. Schematic diagram of biastatic system .....	2
2. Schematic configurations of dynamically unstable system ...	4
3. Schematic representation of biastatic system as a compound pendulum .....	4
4. Variations of $K_1$ , $K_2$ and $-K_2/K_1$ (see text) .....	8
5. General view of the Biastatic Magnetometer at the Geological Survey of Canada .....	12
6. Close up view of specimen holder .....	14
7. Variation of $\alpha/\xi$ (see text) .....	19
8. Ranges of measurable intensities at different sensitivity settings.....	26



#### ABSTRACT

The widely used 2-magnet, Blakett-type astatic magnetometer cannot be used efficiently for Palaeomagnetic research in laboratories where the ambient magnetic field and its vertical gradient are subject to constant variations. It is shown that under such conditions, the 3-magnet or "biastatic" magnetometer is theoretically more stable and adequate. Considerations for the design of such an instrument are briefly reviewed and a description is given of an instrument of this type developed at the Geological Survey of Canada. An important feature of this instrument is that its operation can be carried out automatically. The results obtained in testing the performance of the instrument are analyzed.



INTRODUCTION

Simple or 2-magnet astatic magnetometers are very commonly used for measuring the weak remanent magnetic moments of small rock specimens. Useful considerations for the design of these instruments have been given by many authors among whom Blackett (1952) is probably the one who wrote most comprehensively on the subject. Very high sensitivity has been achieved with instruments of this type, although it is known that their stability is readily disturbed by ambient earth's field fluctuations and this may even preclude their use under otherwise very suitable laboratory conditions. Because the 3-magnet or "biastatic" system is theoretically less responsive to magnetic field fluctuations, its adoption in magnetically noisy environments was long ago suggested by Forrer (1929) and by Thellier (1938). The description of a more recent biastatic magnetometer was given by Pozzi and Thellier (1963).

Most of the literature on astatic magnetometers stresses the high sensitivity and the high signal-to-noise ratio of these instruments as the important criteria for adequacy while relatively little has been written concerning the automation of the measurements. The instrument described by DeSa (1963) is probably an exception to the rule. Although this aspect may be of secondary scientific interest only, its importance is gradually gaining momentum among workers in the field of palaeomagnetism because of the large number of measurements inherent in this type of work.

A biastatic automatic magnetometer was developed in the laboratories of the Geological Survey of Canada. The objectives set at the beginning of this development were to achieve an automatic instrument of good stability and relatively high sensitivity. Major considerations in the design of the instrument will be discussed in this paper and a description of the instrument will be given along with an analysis of its performance.

PART I

THEORETICAL CONSIDERATIONS

A schematic representation of a biastatic system is given in Figure 1. Magnets  $p_1$  and  $p_2$  are theoretically of equal magnetic moments, parallel to each other and antiparallel to magnet  $p_0$ , whose magnetic moment



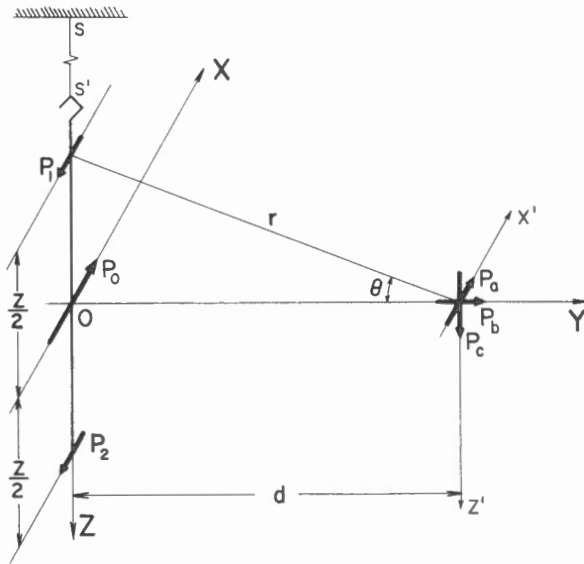


Figure 1: Schematic diagram of biastatic system.

is twice that of either  $p_1$  or  $p_2$ . The three magnets are mounted on a rigid stem whose upper extremity is suspended from a fixed point S by a torsion fiber  $SS'$ . Oscillations of the system about its longitudinal axis may be damped electro-magnetically by means of either a copper plate or a small shorted coil appropriately located in the vicinity of one of the magnets.

The equilibrium of the system may be disturbed by either one or a combination of the following external causes: ambient magnetic field fluctuations, sharp disturbances of the point S of suspension, laboratory air temperature variations and the building up of electrostatic charges in the vicinity of the freely suspended system. A brief discussion on the vulnerability of the system's equilibrium to each of these sources of noise will precede an analysis of the system's limit of resolution.

#### Stability of the biastatic system

In the following discussion we shall denote by  $\sigma$  (dynes cm/radian) the restoring torque constant of the torsion fibre, by H (Oersteds) the horizontal component of the earth's field at point O and by  $\Delta H$  (Oersteds) the

linear increment of H from  $p_2$  to  $p_1$  (Fig. 1). We shall assume further that  $\partial^2 H / \partial z^2$  and the higher order derivatives of H along the vertical are negligible. The magnetic equilibrium of the system is then defined by:

$$(1.1) \quad \vec{p}_1 \times \left( \vec{H} + \frac{\Delta \vec{H}}{2} \right) + \vec{p}_2 \times \left( \vec{H} - \frac{\Delta \vec{H}}{2} \right) + \vec{p}_0 \times \vec{H} - \vec{\sigma} \varphi = 0$$

where  $\varphi$  is the angle of twist of the torsion fibre.

If the system is perfectly astaticized, i.e. if

$$\vec{p}_1 + \vec{p}_2 + \vec{p}_0 = \Delta_1 \vec{p} = 0$$

and

$$\vec{p}_1 - \vec{p}_2 = \Delta_2 \vec{p} = 0$$

then  $\varphi = 0$ , independently of the values of H and  $\Delta H$ . However, since both H and  $\Delta H$  are assumed to vary with time, deviations of the system from perfect astaticism will make  $\varphi$  a function of time which may be defined by

$$(1.2) \quad \vec{\sigma} \varphi_3(t) = t \Delta_1 \vec{p} \times \left( \frac{d\vec{H}}{dt} + \frac{t}{2} \frac{d^2 \vec{H}}{dt^2} + \dots \right) + t \Delta_2 \vec{p} \times \left[ \frac{d}{dt} \left( \frac{\Delta \vec{H}}{2} \right) + \frac{t}{2} \frac{d^2}{dt^2} \left( \frac{\Delta \vec{H}}{2} \right) + \dots \right]$$

The corresponding function  $\varphi_2(t)$  for the 2-magnet system would be expressed as:

$$(1.3) \quad \vec{\sigma} \varphi_2(t) = t \Delta \vec{p} \times \left( \frac{d\vec{H}}{dt} + \frac{t}{2} \frac{d^2 \vec{H}}{dt^2} + \dots \right) + t \vec{p} \times \left[ \frac{d}{dt} (\Delta \vec{H}) + \frac{t}{2} \frac{d^2}{dt^2} (\Delta \vec{H}) + \dots \right]$$

where  $\vec{p}$  and  $\Delta \vec{p}$  are the magnetic moment of each of the magnets and their vectorial sum respectively. In the general case where H and  $\Delta H$  fluctuate, the biastatic system is more stable than the simple astatic system because  $\Delta_2 p$  will normally be much smaller than  $2p$  and  $\Delta_1 p$  may be reduced to the

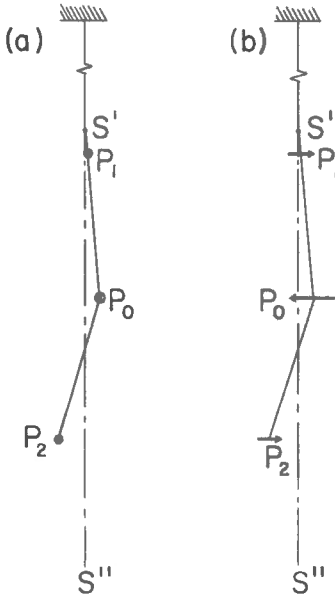


Figure 2. Schematic configurations of dynamically unstable system.

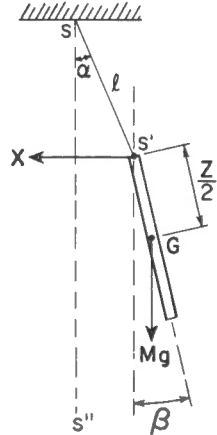


Figure 3. Schematic representation of biastatic system as a compound pendulum.

same order of magnitude as  $\Delta p$ . A high degree of astaticism may be considered as the first condition of stability of either system. A second condition is that the magnets be accurately centred along the axis of the stem and that their magnetic dipoles be rigorously in the same plane. Small departures from this condition will yield either one or a combination of the configurations schematically represented in Figure 2.

Variations in H and/or horizontal displacements of point S occasioned by mechanical noise in the building will be transmitted to the system and affect its stability. Finally, an obvious condition for long term stability is that the material of which the magnets are made be magnetically stable. This implies that the material be resistant to oxidation and that temperature fluctuations of the order of those which are to be expected in a laboratory have no appreciable effect on its remanent magnetization.

The biastatic system may also be looked upon as a compound pendulum, as represented schematically in Figure 3. Using the nomenclature of this sketch and assuming that both angles  $\alpha$  and  $\beta$  are always small, we may write:

$$(1.4) \quad M k^2 \frac{d^2 \beta}{dt^2} = \frac{X Z}{2} - \frac{M g Z}{2} \beta$$

where "k" is the radius of gyration of the system relative to point G, its centre of gravity, and M is its mass. We may also write

$$(1.5) \quad M \left( \frac{\ell d^2 \alpha}{dt^2} + \frac{Z d^2 \beta}{2 dt^2} \right) = - X$$

and

$$(1.6) \quad X \ell = M g \alpha$$

from which we get

$$(1.7) \quad k^2 \frac{d^2 \beta}{dt^2} + \frac{Z}{2} \left( \frac{\ell d^2 \alpha}{dt^2} + \frac{Z d^2 \beta}{2 dt^2} \right) + \frac{g Z \beta}{2} = 0$$

and

$$(1.8) \quad \ell \frac{d^2 \alpha}{dt^2} + \frac{Z}{2} \frac{d^2 \beta}{dt^2} + g \alpha = 0$$

Setting next  $\alpha = A \cos (nt + \epsilon)$

and  $\beta = B \cos (nt + \epsilon)$

we may rewrite (1.7) and (1.8) in the form

$$(1.9) \quad \left[ n^2 \left( k^2 + \frac{Z^2}{4} \right) - \frac{g Z}{2} \right] \beta + \frac{Z \ell n^2 \alpha}{2} = 0$$

and

$$(1.10) \quad \alpha = n^2 Z \beta / 2 (g - \ell n^2)$$

$$\text{or (1.11) } \ell k^2 n^4 - \left( k^2 + \frac{Z^2}{4} + \frac{Z\ell}{2} \right) gn^2 + \frac{g^2 Z}{2} = 0$$

Solving for  $n^2$  yields

$$(1.12) \quad n^2 = \frac{g}{2k^2\ell} \left[ \left( k^2 + \frac{Z^2}{4} + \frac{Z\ell}{2} \right) \pm \sqrt{\left( k^2 + \frac{Z^2}{4} + \frac{Z\ell}{2} \right)^2 - 2Zk^2\ell} \right]$$

from which we may express the two pendulous modes of the system by

$$v_1 = \frac{1}{2\pi} \sqrt{n_+^2} \quad \text{and} \quad v_2 = \frac{1}{2\pi} \sqrt{n_-^2}$$

If we assume next that the point of suspension S undergoes an oscillation of frequency  $v_0$  and amplitude  $\xi_0$ , we may derive that the amplitude of point G is given by

$$(1.13) \quad x = \frac{v_1^2}{(v_1^2 - v_0^2)} \xi_0$$

As disturbance of point S may equally well trigger torsional and pendulous oscillations in the system, it is dually important to mechanically decouple this point from the laboratory floor.

Slow temperature variations of the ambient atmosphere may occasion variations in the torsion constant of the suspension strip and in the resistivity of the electromagnetic damping mechanism. These variations may compensate each other partly and their net effect over the period of time required for the measurement of a specimen may be regarded as part of the instrumental drift. On the other hand, discrete and rapid thermal fluctuations within the system constitute a less tangible source which may be referred to as thermal noise. Blackett (1952) shows that the r.m.s. angular displacement  $\gamma_0$  resulting from this source may be expressed as

$$(1.14) \quad \gamma_0 = \frac{\epsilon^{1/2} T}{2\pi I^{1/2}} \quad \text{radians}$$

where  $\epsilon$  stands for the product of Boltzmann's constant by the absolute temperature and is equal to  $4 \times 10^{-14}$  at  $17^\circ\text{C}$ , T is the undamped period of the system and I is its moment of inertia. Whereas the thermal drift may be kept low by controlling the laboratory temperature, the thermal noise must

be accepted as a factor limiting the resolution of the instrument. It is noted, however, that this factor will generally be negligible compared with noises originating in the other sources mentioned earlier.

Finally, an astatic system may behave somewhat like a Coulomb balance if an electrically charged, although not necessarily a magnetic body is brought in its vicinity. In practice this condition may result from the friction of the different parts of the specimen holder. This source of noise is rather easily circumscribed however by properly shielding the magnetometer casing and by grounding the torsion strip.

Limit of resolution of the biastatic system

As the biastatic system is to serve as a quantitative detector, it is important to define clearly its response to the added presence of a dipole  $\vec{P} = \vec{P}_a + \vec{P}_b + \vec{P}_c$  (Fig. 1) at point (0, d, 0). Expressions for the x and y components of the magnetic field resulting from the dipole at  $p_0$ ,  $p_1$  and  $p_2$  respectively are listed in Table I.

TABLE I

Expression of fields at  $p_0$ ,  $p_1$  and  $p_2$  due to Dipole P

Points	$H_x$	$H_y$
$p_1$	$- P_a/r^3$	$\left[ P_b (3 \cos^2 \theta - 1) + 3P_c \sin 2\theta/2 \right] /r^3$
$p_0$	$- P_a/d^3$	$2 P_b/d^3$
$p_2$	$- P_a/r^3$	$\left[ P_b (3 \cos^2 \theta - 1) - 3P_c \sin 2\theta/2 \right] /r^3$

The effect of the dipole is to shift the equilibrium position of the system by an angle  $\gamma$  which is defined by

$$(2.1) \quad \Delta_1 \vec{p} \times \vec{H} + \Delta_2 \vec{p} \times \left[ \frac{\Delta \vec{H}}{2} + \frac{3 P_c \sin 2 \theta}{2 r^3} \frac{\vec{P}_b}{P_b} \right] +$$

$$(\vec{P}_1 + \vec{P}_2) \times \left[ \vec{P}_b (3 \cos^2 \theta - 1) / r^3 - \vec{P}_a / r^3 \right] + \vec{p}_o \times \left[ \frac{2 \vec{P}_b}{d^3} - \frac{\vec{P}_a}{d^3} \right] - \vec{\sigma} (\varphi + \gamma) = 0$$

Assuming that the system is perfectly astatized (i.e.  $\Delta_1 p = \Delta_2 p = \varphi = 0$ ) and that  $\gamma$  is small, we may write

$$(2.2) \quad P_o P_b \left[ (3 \cos^2 \theta - 1) / r^3 - 2 / d^3 \right] - \gamma P_o P_a \left( \frac{1}{d^3} - \frac{1}{r^3} \right) + \sigma \gamma = 0$$

or (2.3)  $\gamma \sigma = \frac{-P_o}{d^3} (P_b K_1 - P_a K_2 \gamma)$

where  $K_1 = (3 \cos^2 \theta - 1) \cos^3 \theta - 2$  and  $K_2 = (1 - \cos^3 \theta)$ . The variations of  $K_1$ ,  $K_2$  and  $-K_1/K_2$  with  $\cos \theta$  are represented in Figure 4. It is noted that  $K_1$  reaches its maximum absolute value of 2.036 when  $\cos \theta = \sqrt{5}/5$  or  $z = 4d$ ,

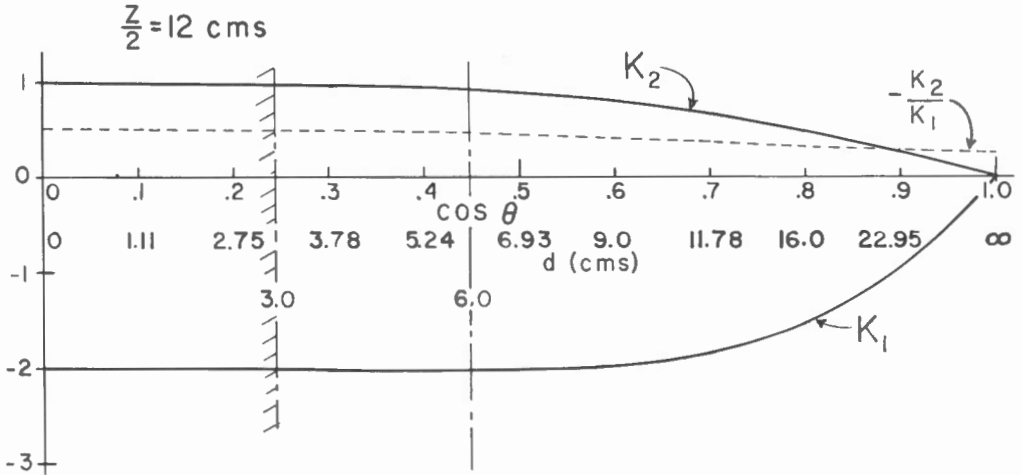


Figure 4. Variations of  $K_1$ ,  $K_2$  and  $-K_2/K_1$  (see text)

for which  $K_2$  equals 0.911. Since  $\gamma$  is small, the product  $K_2\gamma$  may generally be considered negligible compared to  $K_1$  and, in the particular case where  $P_a$  and  $P_b$  are of the same order of magnitude we may write

$$(2.4) \quad \gamma \doteq - \frac{P_o P_b}{\sigma d^3} K_1$$

as a first approximation.

If we define next  $\gamma_m$  and  $P_{bm}$  as the minimum detectable values of  $\gamma$  and  $P_b$  respectively, we may express the limit of resolution of the system by

$$(2.5) \quad P_{bm} = \frac{-\sigma d_m^3 \gamma_m}{P_o K_{1m}}$$

where  $K_{1m}$  is the value of  $K_1$  for  $d = d_m$ , the shortest distance that may physically separate the centre of the dipole  $P$  from the axis of the magnet system.

A derivation parallel to the above for the simple astatic system would yield

$$P_{cm} = \frac{\sigma d_m^3 \gamma_m}{P_o K_{om}}$$

where  $K_o = 3 \sin(2\theta) \cos^3(\theta)$  which reaches a maximum value of 1.7 when  $d$  equals  $z$ .

We may next consider the effect of adding to the simple dipole  $P$  an induced dipole  $C$  whose intensity is proportional to the ambient field at  $(0, d, 0)$ . The two horizontal components of  $C$  may be expressed as

$$C_{x'} = \left( H_{x'} - \frac{P_o \cos \gamma K_2}{d^3} \right) k_{x'} v$$

$$C_y = \left( H_y - \frac{P_o \sin \gamma K_1}{d^3} \right) k_y v$$

where  $v$  is the volume of the specimen,  $k_{x'}$  and  $k_y$  its susceptibilities in the  $X'$  and  $Y$  directions respectively and  $H_{x'}$  and  $H_y$  the horizontal components of the earth's magnetic field at  $(0, d, 0)$ .



In order to simplify matters we may assume for the present discussion that  $H_{x'}$  and  $H_y$  are zero at  $(0, d, 0)$  since in practice this condition is easily achieved to a close approximation with a system of Helmholtz coils centred on this point. Equation (2.3) then becomes

$$(2.6) \quad \gamma \sigma = \frac{-P_o}{d^3} \left[ (P_b + C_y) K_1 - (P_a + C_{x'}) K_2 \gamma \right]$$

It is possible to derive 23 other equations of the form of equation (2.6) by assigning to the dipole the other orthogonal positions in which it may be oriented. We may choose for this discussion the four positions which would result from first placing the dipole in the position given in Figure 1 and then rotating it consecutively by  $180^\circ$  once about the  $X'$  axis, then about the  $Y$  axis and again about the  $X'$  axis. The system of equations defining  $\gamma$  in those cases could be expressed as:

$$(2.7-a) \quad \gamma_1 = \frac{-P_o}{od^3} \left[ K_1 \left( P_b - \frac{P_o \sin \gamma_1 K_1 k_y v}{d^3} \right) - K_2 \left( P_a - \frac{P_o \cos \gamma_1 K_2 k_{x'} v}{d^3} \right) \gamma_1 \right]$$

$$(2.7-b) \quad \gamma_2 = \frac{-P_o}{od^3} \left[ K_1 \left( -P_b - \frac{P_o \sin \gamma_2 K_1 k_y v}{d^3} \right) - K_2 \left( P_a - \frac{P_o \cos \gamma_2 K_2 k_{x'} v}{d^3} \right) \gamma_2 \right]$$

$$(2.7-c) \quad \gamma_3 = \frac{-P_o}{od^3} \left[ K_1 \left( -P_b - \frac{P_o \sin \gamma_3 K_1 k_y v}{d^3} \right) - K_2 \left( -P_a - \frac{P_o \cos \gamma_3 K_2 k_{x'} v}{d^3} \right) \gamma_3 \right]$$

$$(2.7-d) \quad \gamma_4 = \frac{-P_o}{od^3} \left[ K_1 \left( P_b - \frac{P_o \sin \gamma_4 K_1 k_y v}{d^3} \right) - K_2 \left( -P_a - \frac{P_o \cos \gamma_4 K_2 k_{x'} v}{d^3} \right) \gamma_4 \right]$$

Assuming again that  $\gamma_i$  is small enough to permit writing  $\sin \gamma_i \doteq \gamma_i$  and  $\cos \gamma_i \doteq 1$ , we may combine the four equations to yield

$$(2.8-a) \quad \gamma_1 - \gamma_2 = \frac{-P_o}{od^3} \left[ 2K_1 P_b - (\gamma_1 - \gamma_2) K_2 P_a + (\gamma_1 - \gamma_2) \frac{P_o v}{d^3} \left( K_2^2 k_{x'}^2 - K_1^2 k_y^2 \right) \right]$$

$$(2.8-b) \quad \gamma_4 - \gamma_3 = \frac{-P_o}{od^3} \left[ 2K_1 P_b + (\gamma_4 - \gamma_3) K_2 P_a + (\gamma_4 - \gamma_3) \frac{P_o v}{d^3} \left( K_2^2 k_{x'}^2 - K_1^2 k_y^2 \right) \right]$$

which may finally be combined to yield

$$(2.9) \quad P_b = \frac{1}{4K_1} \left[ -\frac{\sigma d^3}{P_0} (\gamma_1 + \gamma_4 - \gamma_2 - \gamma_3) + (\gamma_1 - \gamma_2 + \gamma_3 - \gamma_4) K_2 P_a + \right. \\ \left. (\gamma_1 + \gamma_4 - \gamma_2 - \gamma_3) \frac{P_0 v}{d^3} (K_1^2 k_y - K_2^2 k_{x'}) \right]$$

The last equation points to the theoretical prerequisite knowledge of  $P_a$ ,  $k_x$ , and  $k_y$  for the determination of  $P_b$ . However, it will be shown in the second part of this paper that the middle term may always be neglected and if  $k_x$  and  $k_y$  are smaller than  $10^{-3}$  cgs, the last term in brackets may also be neglected. The equation thus reduces to

$$(2.10) \quad P_b \doteq \frac{1}{4K_1} \left[ -\frac{\sigma d^3}{P_0} (\gamma_1 + \gamma_4 - \gamma_2 - \gamma_3) \right]$$

## PART II

### THE GEOLOGICAL SURVEY INSTRUMENT

#### Description

The instrument has been in operation for the last three years on the fifth floor of the Geological Survey Building which is located in the centre of the City of Ottawa. The eight floor building has a steel beam framework and it shelters various types of laboratories from which may emanate sporadic magnetic fields. The three elevators which are in regular operation during working hours less than 40 metres away from the magnetometer contribute to the various sources of magnetic noise which may be detected in the laboratory where the magnetometer is installed. Because of these relatively adverse conditions a 3-magnet rather than a 2-magnet astatic system was prescribed in the design of the instrument.

The mechanical stability of the building has not been thoroughly investigated by the writers but it is easy to imagine that a certain amount of mechanical noise is transmitted to the laboratory floor from heavy street traffic in the vicinity or from the operation of various types of machinery in other parts of the building. Other major elements of noise detected in the laboratory are caused by strong winds, corridor traffic, etc. For these reasons, a vibration-free stand was considered to be an essential part of the instrument.



Figure 5. General view of the Biastatic Magnetometer at the Geological Survey of Canada.

A system of three mutually perpendicular sets of pseudo-Helmholtz coils is centred about halfway between the magnetometer's axis and the point defined by  $(0, d_m, 0)$  in (2.5). With the appropriate currents circulating through these sets of coils the three components of the magnetic field at the specimen holder are kept less than 50 gammas.

A mechanism for the automatic recording of  $\gamma_i$  is incorporated in the optical system in order to reduce the chances of human error and to make the operation less tedious, faster and more uniform.

A general view of the instrument is given in Figure 5. The components of the instrument which characterize it more specifically are its specimen holder, its biastatic system, its automatic recording system, its multi-sensitivity and damping systems and its anti-vibration set-up. A more detailed description of these components will be given next.

Specimen holder This (Fig. 6) was originally designed to accept cubic specimens 2.54 cm on a side or cylinders 3.17 cm in diameter by 2.86 cm in length, but smaller specimens may also be centred in it by means of appropriate adapters conforming to these dimensions.

The specimen holder is made of aluminum, lucite and bakelite which have been tested for non-magnetic characteristics. Its dual functions are (1) to rotate the specimen about the vertical and about a precessing horizontal axis in order to make it assume various orthogonal positions, and (2) to centre the specimen along the Y axis at an appropriate distance from the Z axis. The two operations are motor driven and may therefore be triggered by remote controls. The exact orientation of the specimen in each of its orthogonal positions is made possible by means of a magnetic clutch which disengages the drive shaft of the specimen holder from the motor as soon as the current is cut off. This occurs when a protruding point on the drive shaft actuates a limiting switch as the specimen reaches a new orthogonal position. An operator remote from the magnetometer may actuate a spring loaded switch which by-passes the limiting switch for about one second while the motor is being started for the next positioning operation. The orienting mechanism is free to travel along the Y axis in the range  $6 \leq d \leq 36$  cm and the to and fro motion is governed by two lead screws which are powered by a reversible electric motor. In order to avoid interference of the motors with the astatic system operation, the two motors are located about 5 metres away from it.

The determination of any one of the three orthogonal components ( $P_a$ ,  $P_b$ ,  $P_c$ ) of remanent magnetization is based on a minimum of four readings which are made when the specimen is lying in four different and specific orthogonal positions. In determining the  $P_c$  component, an additional four readings are made which give the total number of 16 readings for each specimen. The reading obtained while the specimen lies in its first position is repeated after the 16th reading for verification purposes only.

At the beginning of a determination, the specimen is placed in the specimen holder so that its a, b, and c axes are respectively directed along

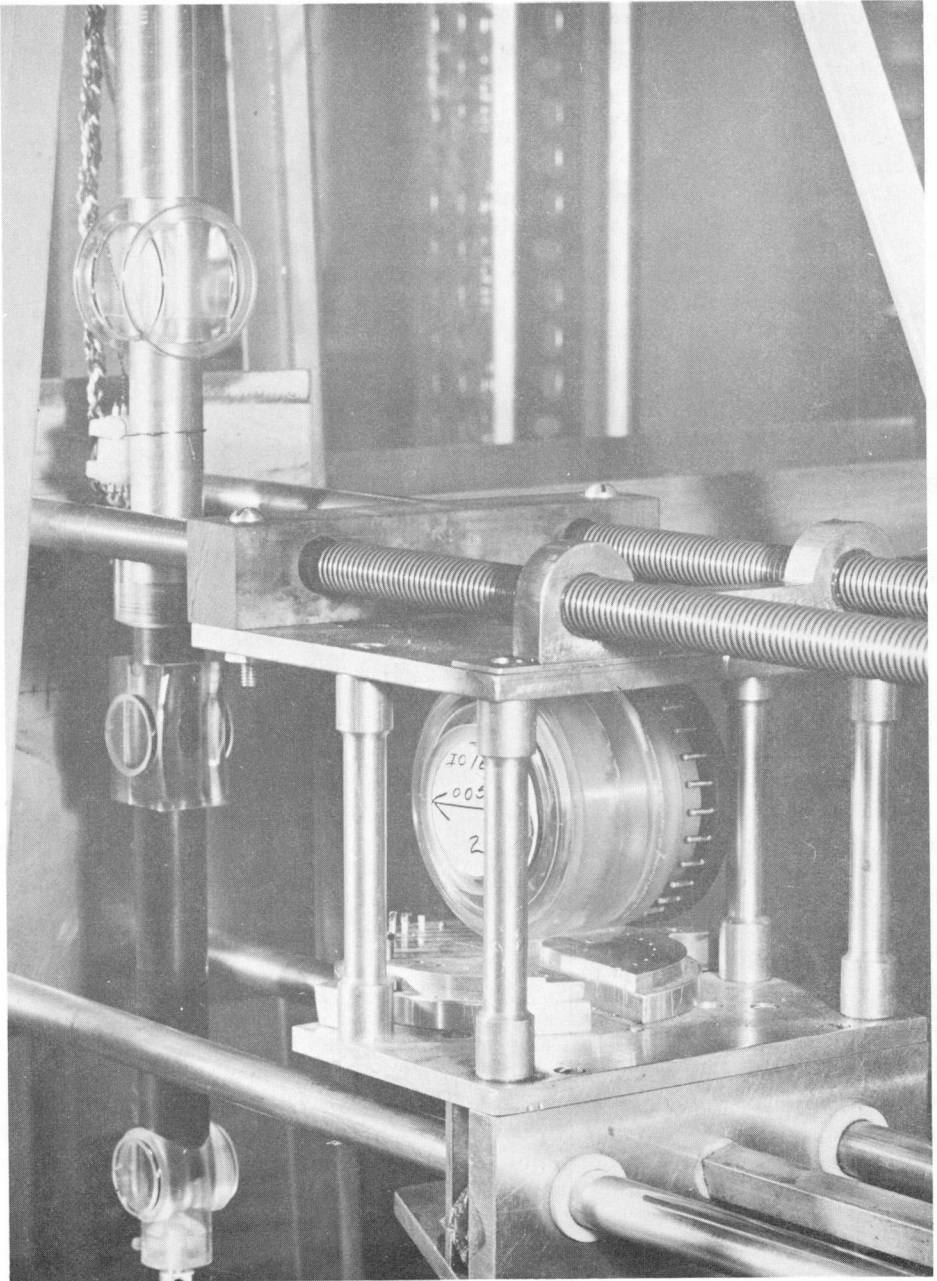


Figure 6. Close up view of specimen holder.

the  $-Z'$ ,  $X'$ , and  $-Y$  directions. Three consecutive  $90^\circ$  rotations about the  $Z'$  axis yield the first four positions defined in Table II. The fifth position is obtained by two simultaneous  $90^\circ$  rotations about the  $Z'$  and the  $c$  axes. Following the same program, it is easy to derive the other positions listed in Table II. It can be verified that the differentials  $(\gamma_{11} - \gamma_1)$ ,  $(\gamma_3 - \gamma_9)$ ,  $(\gamma_{15} - \gamma_5)$  and  $(\gamma_7 - \gamma_{13})$  may be used to determine  $P_c$ , the differentials  $(\gamma_2 - \gamma_{10})$  and  $(\gamma_{12} - \gamma_4)$ , to determine  $P_b$  and the differentials  $(\gamma_6 - \gamma_{14})$  and  $(\gamma_{16} - \gamma_8)$ , to determine  $P_a$ .

Biastatic system The distance  $Z/2$  between the middle magnet and the other two was set at 12 cm so that the parameter  $K_1$  would have its maximum value when  $d = d_m = 6$  cm. The longitudinally magnetized magnets are fitted in holes bored through three small aluminum prisms which are linked by two  $1\frac{1}{2}$  cm long rods, 1.6 mm in diameter. A rectangular plane mirror which is affixed to the top prism in the upright position is a 0.15 mm thick aluminized glass slip 6 mm long by 3 mm wide. The moment of inertia of the assemblage (magnets excluded) was determined experimentally as  $0.014 \text{ g cm}^2$ .

The platinum-cobalt alloy of equiatomic proportions known as PLATINAX II was chosen as the material for the magnets. The diameter of the large magnet is 3.2 mm and its length is 4.6 mm. The corresponding dimensions of the small magnets are 2.5 and 3.7 mm respectively. The measured magnetic moments of the magnets (17.42 and 8.71 cgs units) produce a field of approximately 0.07 oersted in the  $-X'$  direction at point (0, 6, 0). The calculated moments of inertia of the magnets about the axis of the stem are  $0.016$  and  $0.005 \text{ g cm}^2$  respectively, so that the total moment of inertia of the biastatic system is estimated as  $0.04 \text{ g cm}^2$ .

Assuming an undamped period  $T$  of 10 seconds for the system, the r.m.s. value of its thermal noise  $\gamma_0$  is estimated from equation (1.14) as  $1.5 \times 10^{-6}$  radians. On the other hand, considering that the centre line of a one cm wide light spot can with difficulty be located on a scale 3.5 m from the mirror with an accuracy better than  $\pm .25$  mm, it may be calculated with the aid of equation (2.5) that the value of  $\gamma_m$  would be  $3.6 \times 10^{-4}$  radians. The r.m.s. value of the thermal noise is thus significantly smaller than the limit of resolution of the biastatic system.

Automatic recording system The biastatic system angular deflections  $\gamma_i$  are determined optically, much in the same way as the deflections of a sensitive galvanometer. A light beam from a source located 3.5 m away from the middle magnet is reflected from the mirror of the biastatic system onto the locked-in split photocell of a commercially available spot-follower. The output voltage of the spot-follower varies linearly as the position of the

TABLE II - 16 orthogonal positions of dipole P relatively to axes X', Y and Z'

Dipole Component	<u>POSITION No.</u>															
	1	2	3	4	5	6	7	8	9	10	11	12	13	14	15	16
P <sub>a</sub>	-Z'	-Z'	-Z'	-Z'	X'	Y	-X'	-Y	Z'	Z'	Z'	Z'	-X'	-Y	X'	Y
P <sub>b</sub>	X'	Y	-Z'	-Y	Z'	Z'	Z'	Z'	-X'	-Y	X'	Y	-Z'	-Z'	-Z'	-Z'
P <sub>c</sub>	-Y	X'	Y	-X'	-Y	X'	Y	-X'	-Y	X'	Y	-X'	-Y	X'	Y	-X'

photocell along a 21 cm long scale located below the light source and oriented parallel to the Y axis of the magnetometer. This voltage is read and digitized by a digital voltmeter which is hooked up to a matched printing unit. Its range over the length of the scale is from 100 mv to 940 mv so that a displacement of 1 mm of the reflected light beam on the scale produces a 4 mv change in the printed voltage output.

The voltage at the moving contact of a multiple turn potentiometer is used as a measure of the distance between the centre of symmetry of the specimen and the middle magnet. The potentiometer shaft is geared to the lead screws used in positioning the orienting mechanism along the Y axis. The voltage across the potentiometer's terminals and the angular position of the moving contact are adjusted so as to yield a voltage proportional to the distance between the Z and Z' axes. This voltage is in turn digitized and printed, as in the previously described system.

The magnetometer operation is programmed through an electro-mechanical unit from which commands are emitted to the digital voltmeter, the printer and the orienting mechanism. Once the distance between the Z and Z' axes has been adjusted through a manual switch at the console, a trigger switch is actuated to initiate the cycle of operations necessary for the magnetization determination of a specimen. The sequence of operations is as follows:

- a) reading and recording of the voltage corresponding to the distance  $d$ ,
  - b) reading and recording of the voltage corresponding to the angular deflection of the biastatic system while the specimen is in its initial position,
- and c) orientation of the specimen in the next position followed by reading and recording of the voltage corresponding to the magnetometer deflection with the specimen in that position.

This third operation is repeated 15 times after which the specimen is reoriented in its initial position and the corresponding voltage is recorded to verify that the instrument drift during the measurement was not significant. An 18-position multiple deck solenoid operated switch is used to energize the various circuits required for a specific operation and to act as a counter. The synchronized commands, including that of rotating the 18-position switch, are emitted through a series of relays and delay relays. The delays separating the orientation and reading commands are adjustable to a prescribed duration in the range of 0.6 to 60 seconds by means of a variable resistor in the circuit of one of the delay relays.



The multi-sensitivity and damping systems Because the intensity of magnetization of rocks may differ widely from one specimen to the next, it was considered useful to add to the magnetometer a feature which allows the operator to vary its sensitivity rapidly and through a simple operation. For this purpose three small Helmholtz coils centred on and coaxial with each of the magnets respectively are mounted on the magnetometer casing (see Fig. 6). When a current of the appropriate polarity is fed through the coils which are connected in series, their magnetic field tends to oppose any angular deflection of the system, much as if the torsion constant of the suspension strip had been increased. Effectively, the value of  $\sigma$  in (2.10) is modified to  $(\sigma + p_1 H_1 + p_2 H_2 + p_0 H_0)$ , where  $H_1$ ,  $H_2$  and  $H_0$  are the fields at the centres of the coils. A voltage divider controlled through a multipole switch thus allows the operator to set the effective value of  $\sigma$  to 2, 5, 10, 20, 50, 100, 0.5 or 0.2 times its normal value. The last two settings clearly refer to sensitivity increases and are obtained by current reversals in the coils.

Much in the same way as when the torsion constant of the strip is changed, the period of the system is modified and accordingly, an adjustment for critical damping is required after each sensitivity change. The conventional method of damping which consists of positioning a copper disk near the bottom magnet would hardly be suitable for remote control adjustment. Instead, a small Helmholtz coil centred on the upper magnet and axially directed parallel to the Y axis (Fig. 6) is used. The coil is wired in series with a voltage generating device incorporated in the spot-follower. As the split-photocell is carried away in one direction, a voltage proportional to its speed is generated which energizes the damping coil in the direction opposing the movement of the biastatic system. Critical damping is achieved by inserting an appropriate resistance in the damping circuit. Adjustable resistors are inserted in the circuit through a multipole switch which is ganged to the multi-sensitivity switch so that the damping is automatically adjusted to its critical value for each sensitivity setting.

As the period of the system is a function of its sensitivity, the delay between the orientation and reading commands must be adjusted to a specific length for each sensitivity setting. This is achieved by inserting a convenient resistor in the delay relay circuitry for each setting. These resistors are also switched in through the multi-sensitivity switch mentioned above.

Finally, to avoid the possibility of error in recording the sensitivity at which a given determination is done, each setting is coded and the code number is printed opposite the distance record on the output tape.

Anti-vibration precautions Isolating the biastatic system mechanically from the building was achieved partly by mounting the base of the instrument on a heavy pedestal whose inertia is used to dissipate much of the energy of the

vibrations transmitted along the laboratory floor. A half-ton mass of cinder blocks held together in a wooden framework is mounted on five  $25 \text{ cm}^2$  "Isomode" rubber pads which are located at its corners and at its centre respectively.

The base of the instrument consists of a  $1 \frac{1}{4} \text{ cm}$  thick aluminum plate to which is bolted a 50 kg mass of lead. The aluminum plate rests on four isolating pads distributed one at each of its corners. Four converging legs are bolted on the aluminum plate and are linked at the top by a 20 by 20 by 2 cm aluminum plate which is bored at the centre to accept the ring of a gimbals suspension. The inner member of the gimbals is a 10 cm long copper cylinder,  $7 \frac{1}{2} \text{ cm}$  in diameter and with a 2 cm diameter hole bored along its axis. The top of the biastatic system casing is connected to the bottom of the copper cylinder and its lower end is linked to the base plate by a stretched elastic band. From the top of the copper cylinder is erected a 45 cm long bakelite tube. An adjusting screw is threaded through a cap at the top of the bakelite tube. The tapered end of the screw is the point S (Figs. 1 and 2) from which the biastatic system is suspended by means of a 15 cm length of phosphore-bronze strip adjoined to a 45 cm length of fine copper wire. The bakelite tube, the copper cylinder and the biastatic system casing considered as a unit form the mass of a compound universal pendulum free to swing about the gimbals axes. The natural frequency of the freely suspended pendulum is raised to 6.67 cps by the stretched elastic band at its lower end.

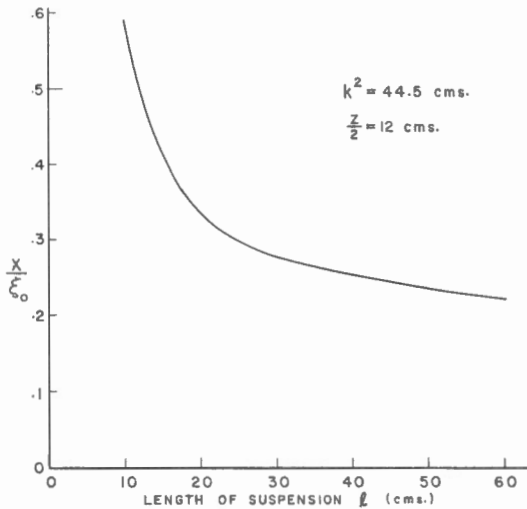


Figure 7. Variation of  $x/\xi$  (see text).

Figure 7 shows the calculated ratio of the amplitude of point G (Fig. 3) to that of point S for various lengths of suspension  $l$ , as determined from equation (1.13). The calculation is based on an estimate of  $\sqrt{44.5}$  cms for the radius of gyration of the biastatic system about the axis of the middle magnet. It appears from these results that, as the length of the suspension strip is increased, the biastatic system becomes less sensitive to horizontal shock waves transmitted to point S and the length of 60 cms selected in the present instrument was found adequate.

### Calibration and operation

The standard used in calibrating the magnetometer is a solenoid 2.2 cm long and 1.33 cm in diameter; the winding comprises 46.2 turns of No. 26 enamel coated copper wire closely wound in one layer over its entire length. For calibration purposes the axis of the solenoid is made to coincide with the Y axis of the instrument and the distance  $d$  between its centre of symmetry and the middle magnet is measured. The magnetic moment of the solenoid seen from the centre of the middle magnet is given by:

$$P_b = \frac{\pi N d^3 i}{10 \ell} \left[ \frac{d - \ell/2}{\left( (d - \ell/2)^2 + a^2 \right)^{1/2}} - \frac{d + \ell/2}{\left( (d + \ell/2)^2 + a^2 \right)^{1/2}} \right]$$

where  $N$  is the number of turns,  $\ell$  and  $a$  are respectively the length and the radius of the solenoid and  $i$  is the current circulating through it. The relative error in measuring the current being less than 1.5% the same relative error is claimed in determining  $P_b$ .

As there are theoretically no  $P_a$  and  $P_c$  components to the solenoid dipole, the use of equation (2.4) is certainly valid in the present discussion. If the current is reversed in two successive observations, we may define the instrument constant  $R$  as follows:

$$R = \frac{2 K_1 P_b}{d^3 (V_1 - V_2)}$$

where  $V_1$  and  $V_2$  are the corresponding output voltages of the spot-follower.

The constant  $R$  was determined for a number of distances  $d$ , the intensity of  $P_b$  being adjusted each time to give the same values of  $(V_1 - V_2)$ .

The results of these calibrations which are listed in Table III show that the constant may be accurately determined independently of the solenoid position along the Y axis, within the practical range of the instrument.

TABLE III - Instrument Constant Determinations for different values of "d"

Distance "d" cms	R x 10 <sup>7</sup>	Distance "d" cms	R x 10 <sup>7</sup>
6	3.94	19	3.96
8	3.97	24	3.92
14	3.98	30	3.94

In order to verify the repeatability of the measurements, a cylindrical rock specimen was placed in the specimen holder and its components of remanent magnetization were determined several times with the instrument adjusted at three different sensitivity settings. The results are listed in Table IV where  $P_a/v$  and  $P_b/v$  refer to the components of magnetization along two mutually perpendicular axes drawn arbitrarily on the end of the cylinder and  $P_c/v$  refers to the component along the axis of the cylinder. The declinations and inclinations listed in Table IV were calculated from these components.

The standard deviation of the intensities of magnetization and that of its a, b, and c components were computed for each of the three groups of readings. These statistics are listed in Table V along with the corresponding mean values. It is noted first that the standard deviations are always lower for the data obtained when the instrument was set at higher sensitivities. This clearly indicates that the precision of the instrument is really increased when it is set at high sensitivities.

It is also noted that the mean intensities were slightly larger when the sensitivity was set at 2X and 5X Normal. This is due to a slight error in the original calibration of the instrument, i. e. the factors 2X and 5X are in reality 2.03X and 5.19X respectively. This discrepancy cannot be considered important as it has no bearings on the angular determinations and it can easily be corrected in the computations of intensities if high precision is required for this type of data.

TABLE IV

Repeated Magnetization Measurements on a 22.6 cc cylindrical specimen at  $d = 6$  cms.

Sensitivity Setting	$P_a/v$ cgs x $10^{-5}/cc$	$P_b/v$ cgs x $10^{-6}/cc$	$P_c/v$ cgs x $10^{-6}/cc$	$P_{total}/v$ cgs x $10^{-5}/cc$	Decl. (degrees)	Incl. (degrees)
Normal	1.256	-3.912	-4.094	1.377	342.7	-17.3
	1.260	-3.821	-4.049	1.378	343.1	-17.1
	1.260	-4.140	-4.208	1.392	341.8	-17.6
	1.256	-3.912	-4.026	1.375	342.7	-17.0
	1.233	-3.776	-3.958	1.349	343.0	-17.1
	1.246	-3.639	-3.867	1.355	343.7	-16.6
	1.228	-3.685	-3.821	1.338	343.3	-16.6
	1.237	-3.594	-3.912	1.347	343.8	-16.9
	1.246	-3.685	-3.730	1.352	343.5	-16.0
	1.233	-3.685	-3.799	1.342	343.4	-16.4
	1.242	-3.685	-3.890	1.353	343.5	-16.7
	1.242	-3.685	-3.776	1.349	343.5	-16.2
	1.265	-3.844	-4.026	1.382	343.1	-16.9
	1.267	-3.844	-4.003	1.383	343.1	-17.1
2 X Normal	1.269	-3.844	-4.071	1.387	343.2	-17.0
	1.262	-3.867	-4.037	1.381	343.0	-16.7
	1.260	-3.799	-3.958	1.374	343.2	-16.7
	1.269	-3.753	-3.981	1.382	343.5	-16.6
	1.265	-3.708	-3.924	1.375	343.7	-16.7
	1.265	-3.730	-3.946	1.376	343.6	-17.0
	1.289	-3.958	-4.112	1.410	342.9	-17.0
	1.294	-3.930	-4.108	1.413	343.1	-16.9
	1.290	-4.031	-4.076	1.412	342.7	-16.8
	1.289	-3.912	-4.067	1.407	343.1	-16.8
	1.291	-4.003	-4.099	1.412	342.8	-16.9
	1.291	-3.958	-4.081	1.411	343.0	-16.8
	1.285	-3.985	-4.058	1.405	342.8	-16.8
	1.289	-3.912	-4.044	1.407	343.1	-16.7

TABLE V - Statistical Parameters of Test Results

Component	Mean Intensities ( $10^{-6}$ cgs/cc)			Standard deviation $10^{-7}$ cgs/cc		
	Normal Sensitivity	2 X Normal Sensitivity	5 X Normal Sensitivity	Normal Sensitivity	2 X Normal Sensitivity	5 X Normal Sensitivity
$P_a/v$	12.449	12.652	12.898	1.103	.3159	.2571
$P_b/v$	3.768	3.798	3.961	1.550	.6079	.4293
$P_c/v$	3.927	3.993	4.089	1.436	.5029	.2432
$P_{total}/v$	13.587	13.801	14.096	1.707	.4476	.2985

TABLE VI - Statistical Angular Parameters of Test Results

Sensitivity	Decl. (Deg)	Incl. (Deg)	Angular Standard	
			Deviation (degrees)	Variance of the 28 determinations (degrees) <sup>2</sup>
Normal	343.17	-16.79	.707	Overall : .2547
2 X Normal	343.30	-16.81	.303	Within-Sample : .2549
5 X Normal	342.94	-16.84	.178	Between-Sample : .2533

The angular standard deviations (Larochelle, 1967) were also computed for each group of data and these statistics are listed in Table VI. It is noted that, from this point of view also, the precision of the instrument is greater as its sensitivity is fully used.

A one-factor angular variance ratio analysis of the data has shown that overall, within-sample and between-sample variances are very nearly identical. This indicates that the mean directions obtained for each group of readings are not significantly distinct and that the mean direction of the 28 observations ( $343.14^\circ$ ,  $-16.81^\circ$ ) is very close to the true direction of magnetization of the specimen.

The intensities of magnetization listed in Table IV were computed on the assumption that the component of magnetization induced into the specimen by the field of the biastatic system was negligible. In fact the susceptibility of the specimen was determined approximately as  $2 \times 10^{-5}$ . We may rewrite equation (2.9) in the form:

$$P_b = \frac{1}{4 K_1} \left[ (A + B) (\gamma_1 + \gamma_4 - \gamma_2 - \gamma_3) + C (\gamma_1 - \gamma_2 + \gamma_3 - \gamma_4) \right]$$

$$\text{where } A = \left| -\frac{\sigma d^3}{P_o} \right|, \quad B = \frac{P_o v}{d^3} \quad (K_1^2 k_y - K_2^2 k_{x'})$$

and  $C = K_2 P_a$ . Setting

$$p_o = 17.42 \text{ cgs units} \quad K_1^2 = 4.14$$

$$d^3 = 216 \text{ cm}^3 \quad K_2^2 = 0.83$$

$$v = 22.6 \text{ cc} \quad k_{x'} = k_y = 2 \times 10^{-5}$$

$$\sigma = 3.6 \times 10^{-3} \text{ degrees cm/rad.}$$

it may be verified that  $B/A \approx .003$ , and thus the parameter B may be ignored in the above equation, in this particular case.

The multiplicands of A and C may be rewritten as (a+b) and (a-b) respectively. In practice a is generally equal to b or nearly so, hence we

may state that in the present case at least, equation (2.10) is a very good approximation of equation (2.9).

The more general case may now be discussed. It is known that the natural remanent magnetization of igneous rocks is nearly always greater than that induced into them by the earth's field. Thus if a specimen has a susceptibility of  $10^{-2}$  cgs units, at least one of its components of natural remanent magnetization should have an intensity of  $5 \times 10^{-3}$  cgs/cc or more. It may be verified from Figure 8 that with a 22.6 cc specimen having an intensity of magnetization of this order, the sensitivity of the instrument would have to be set at N/50 if the centre of the specimen is 6 cm away from the middle magnet. At this setting  $\sigma$  would be equal to about 0.9 dyne cm/radian and the ratio B/A would be approximately  $5 \times 10^{-4}$ . On the other hand, after severe magnetic cleaning treatments have been imposed on the specimen, its remanent magnetization may have decreased by several orders of magnitude while its susceptibility has remained practically unchanged. For the sake of argument, let us suppose that the specimen may now be oriented in any position, 6 cms away from the magnet system, while the instrument sensitivity is set at 2 X Normal. The value of  $\sigma$  is now  $3.6 \times 10^{-2}$  and, accordingly the ratio B/A becomes 0.135. It is clear that in such cases the parameter B can no longer be neglected and that equation (2.10) is a less valid approximation of equation (2.9). This might be an explanation for the observed phenomenon that the directions of magnetization of specimens from the same magnetite bearing sample appear to scatter after alternating field cleaning treatments in high fields (see Larochelle, 1966).

An estimate of the maximum random angular error in determining the direction of magnetization of very weakly magnetized specimens was obtained in the following manner. The sensitivity of the instrument was set at 5 X Normal and the motor normally driving the emptied specimen holder was shut off while the output of the spot-follower was recorded throughout five consecutive regular cycles lasting about 6 minutes each. The sixteen readings recorded during each cycle were considered as the raw data of a regular magnetization determination. The intensity of the "pseudo magnetization vector" corresponding to each set of readings was computed. Out of the five "pseudo vectors", the largest one had a modulus of  $1.1 \times 10^{-6}$  cgs units. Assuming that the volume of the "noise specimen" was 22.6 cc, its intensity of magnetization is calculated as  $4.9 \times 10^{-8}$  cgs units/cc. If this "noise specimen" be superposed on an actual specimen of the same volume and having an intensity of magnetization of  $4.9 \times 10^{-6}$  cgs/cc, the maximum angular error in determining the direction of this magnetization would be given by:

$$\Delta \alpha_{\max} = \arctan (.01) = 0.5 \text{ degree.}$$



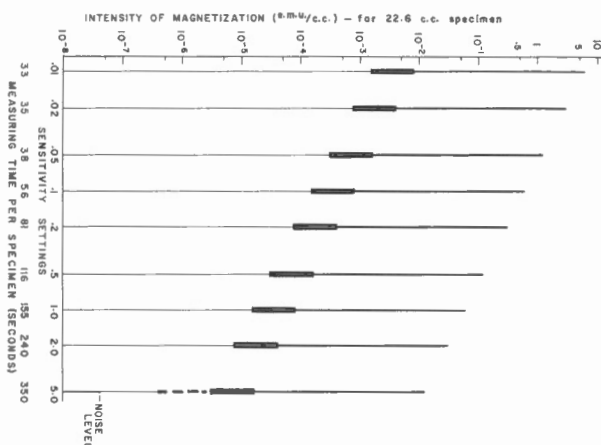


Figure 8. Ranges of measurable intensities at different sensitivity settings. Thick lines indicate ranges of magnetization intensities measurable at the corresponding sensitivity settings. Extra thick lines indicate the same with the restriction that  $d$  equals 6 cms. Ranges calculated on the basis of a 22.6 cc specimen and angular accuracy claimed is  $\pm 1^\circ$  except in dotted line range where the maximum error is  $\pm 6^\circ$ .

The fact that this angle which is given as an estimate of the maximum error is exceeded by the .703 degree angular standard deviation reported in Table VI is not significant since the full sensitivity of the instrument was purposely not used in obtaining the data from which this standard deviation was computed. It is noted on the other hand that the angular standard deviation computed from the data obtained when the sensitivity of the instrument was fully used is appreciably less than .5 degree and that the order of magnitude of the magnetization of the specimen used in that test is the same as that postulated in the present discussion. Using the same reasoning as above, it may be verified that if the intensity of magnetization of the specimen had been  $4.9 \times 10^{-7}$  gcs/cc, the maximum angular error in determining its direction would have been slightly less than 6 degrees. It is obvious that the maximum error would have been still larger for a smaller specimen. Therefore, it seems reasonable to state that if the intensity of magnetization of a 22.6 cm<sup>3</sup> specimen is  $6 \times 10^{-7}$  gcs units/cc or larger, the direction of its magnetization may be determined with an accuracy of  $\pm 5$  degrees. If the intensity is of the order of  $3 \times 10^{-6}$  gcs/cc, an accuracy of  $\pm 1$  degree may be obtained.

The very weak magnetization of the specimen holder is not perceptible by the biastatic system at low sensitivity settings but a few mm displacements of the spot are observed on the scale at the 5 X Normal setting when the empty specimen holder is rotated. However, as these displacements

are systematically distributed during a complete cycle, it is easy to correct for them in computing accurately the magnetization of very weakly magnetized specimens.

The fact that the operation of the instrument is considerably simplified through the various automatic mechanisms incorporated in it reflects on the speed at which a complete determination may be carried out with the present instrument. It is noted however that the time required for a determination depends on the sensitivity setting of the instrument for that particular determination. Figure 8 gives the ranges of magnetization intensities which may be determined with good accuracy at the different sensitivity settings of the instrument and the corresponding durations of a complete determination. Within each range the maximum angular error is one degree and within an extension of the 5 X Normal setting (shown as a broken line) a maximum 5 degree error is claimed.

#### SUMMARY AND CONCLUSION

The instrument described is not presented as a definitive version to its numerous predecessors but rather as one which is believed to be adequate for reliable paleomagnetic determinations, and which differs substantially from astatic magnetometers described so far in the literature. The noise signal of the instrument was shown to be relatively small considering the somewhat adverse conditions of the laboratory in which the measurements were made. The sensitivity of the system is sufficient to cover the useful range of paleomagnetic intensities and the repeatability of the readings obtained during a test suggest that the direction and the intensity of remanent magnetization of a specimen may be determined accurately with this instrument. The multi-sensitivity feature of the apparatus extends its usefulness considerably and the automatic recording of the readings renders the observations more reliable and faster and the readings easily amenable to electronic computer processing.

#### ACKNOWLEDGMENTS

The writers are indebted to Mr. G.M. Meilleur for useful suggestions during the development of the instrument and for his supervising of the shopwork in the machining of the specimen holder and of the biastatic system. The valuable contribution of Dr. E.H.S. Gaucher, formerly of the Geological Survey, in the early stages of the automation is duly acknowledged.

BIBLIOGRAPHY

Blackett, P.M.S.

- 1952: A negative experiment relating to magnetism and the earth's rotation. Phil. Trans. Roy. Soc. London, Ser. A, No. 897, vol. 245, pp. 309-370.

De Sa, A.

- 1963: Application of electronics to the measurement of geophysical phenomena. Unpub. Ph.D. Thesis, University of Durham.

Forrer, R.

- 1929: Sur la structure de l'aimant atomique dans les corps ferromagnétiques. J. de Phys., vol. 7, p. 247.

Larochelle, A.

- 1966: Palaeomagnetism of the Abitibi Dyke Swarm. Can. J. Earth. Sci., vol. 3, pp. 671-683.

- 1967: A re-examination of certain statistical methods in palaeomagnetism. Geol. Surv. Can., Paper 67-18.

Pozzi, J-P. et Thellier, E.

- 1963: Sur des perfectionnements récents apportés aux magnétomètres à très haute sensibilité-utilisés en minéralogie magnétique et en paléomagnetisme. Comptes Rendus Acad. Sci. Paris, vol. 257, No. 5, pp. 1037-1040.

Thellier, E.

- 1938: Sur l'aimantation des terres cuites et ses applications géophysiques. Ann. Inst. Phys. du Globe, vol. 16, pp. 157-302.